ELSEVIER

Journal of Hydrology 257 (2002) 212–225

Journal of Hydrology

www.elsevier.com/locate/jhydrol

Evaluation of basin-scale hydrologic response to a multi-storm simulation

Z. Yu[a,*], E.J. Barron[b], B. Yarnal[b], M.N. Lakhtakia[b], R.A. White[b], D. Pollard[b], D.A. Miller[b]

[a]*Department of Geoscience, University of Nevada Las Vegas, 4505 Maryland Parkway, Las Vegas, NV 89154, USA*
[b]*Earth System Science Center and EMS Environment Institute, Pennsylvania State University, University Park, PA 16802, USA*

Received 15 March 2001; revised 20 July 2001; accepted 12 October 2001

Abstract

Understanding how hydrologic systems of large river basins respond to atmospheric forcing is crucial to regional climate and hydrology studies. A hydrologic model system (HMS) was linked to a regional climate model (RCM) to model a series of storm events passing over the Susquehanna River Basin and to simulate various hydrologic processes in soil hydrology, land surface hydrology, and ground-water hydrology using observed and modeled storm events. The RCM is designed to link to general circulation models and to provide fine spatiotemporal output for hydrologic and other applications. The hydrologic models were calibrated to the observed data (e.g. soil moisture and streamflow) at the basin and subbasin-scales. The HMS-simulated hydrologic response to observed precipitation from a six-storm sequence compares well to the observed. The subgrid-scale spatial variability in precipitation and hydraulic conductivity is included in HMS simulations with RCM-modeled precipitation. Nested 108–36–12 km RCM domains are used for the multi-storm simulation. The 12 km RCM-modeled precipitation is then downscaled to a 1 km hydrologic grid resolution for HMS simulation. Simulations of the six-storm sequence by the RCM produce precipitation fields that appear realistic in general, but that diverge in detail from observed precipitation in both time and space. HMS proves to be sensitive to these details, so the simulated streamflow does not accurately reproduce observed streamflow. The results suggest potential value in improving on the current versions of RCM and HMS for regional climate and hydrology system modeling.

Keywords: Climate models; Hydrologic modeling; Storm simulation; Downscaling

1. Introduction

Dynamic downscaling describes a set of techniques that use dynamic (RCMs) to transform global-scale atmospheric information into higher resolution weather and climate data (e.g. Kattenberg et al., 1996). The motivation for dynamic downscaling is that the data from global-scale observations and general circulation models (GCMs) are too coarse for many regional and local problems.

One of the most important applications of dynamical downscaling is to basin-scale hydrologic modeling. Research to date has pursued one of the two strategies. One approach was to embed an RCM in a GCM and then to direct the relatively high-resolution output to a hydrologic model (Leung et al., 1996). Such one-way linkages were used to simulate streamflow on time scales of months or longer in response to

* Corresponding author. Tel.: +1-702-895-2447; fax: +1-702-895-4064.
E-mail address: zhongbo@nevada.edu (Z. Yu).

0022-1694/02/$ - see front matter
PII: S0022-1694(01)00538-8

El Nino-Southern Oscillation and greenhouse-gas forcing (Leung et al., 1999; Leung and Ghan, 1999, respectively). The other strategy was to simulate individual precipitation events and their hydrologic response by linking a mesoscale meteorological model to a hydrologic model (e.g. Miller and Kim, 1996). Use of two-way interactive nests in the mesoscale model can generate precipitation with fine-scaled grid increments of 4 km and hydrologic responses of hours (Yu et al., 1999a,b).

These two strategies for the dynamic downscaling of various meteorological parameters provide an important base for basin hydrology applications. The previous study (Yu et al., 1999a) on the single storm event leave an important temporal gap, especially in the context of extreme events. Although catastrophic floods can result from single storms or from long-term wet conditions, they commonly arise from a succession of storms often occurring over weeks to months. The hydroclimatology of the Midwest flood of 1993, for instance, falls in this time scale (Kunkel, 1996). Thus, dynamic techniques for hydrologic simulations should be developed for periods ranging from two storms to many storms. This research is part of a plan to bridge this gap.

The study focuses on modeling the hydrologic response to precipitation generated by a six-storm dynamic downscaling simulation with an RCM. The two objectives are to determine how well a system of hydrologic models simulates observed streamflow and then to use that model system to evaluate how well an RCM simulates precipitation over time and space. The methods and results of the dynamic downscaling simulation are summarized here. The following sections consist of the RCM and the hydrologic model system (HMS), of subgrid-scale spatial variability, of the study area and hydrologic data sets, and of model calibration. We then present the results obtained using observed and RCM-modeled precipitation and draw conclusions.

2. Regional climate model (RCM)

For applications involving longer-term simulations, the RCM was modified from the Penn State/NCAR mesoscale meteorological model (also known as MM5) (Dudhia, 1993; Grell et al., 1995). MM5 is a three-dimensional, primitive-equation mesoscale meteorological mode. It is capable of simulating and predicting a large variety of atmospheric phenomena, and of producing high-resolution, four-dimensional, dynamically consistent data sets. It allows the choice of hydrostatic or non-hydrostatic modes, multiple movable nested domains, one-way and two-way interactive nesting procedures, and several different physical process parameterization routines. The model can be used with realistic topography and observational data to create its initial and temporally variable lateral boundary conditions.

The non-hydrostatic capability and the multiple movable nested domain capability make MM5 an extremely versatile model. Mesoscale model simulations with grid increments below ~10 km mean, with very few exceptions, that the model be non-hydrostatic. The nested domain capability allows the use of higher resolution over a particular region of the domain and lower resolution elsewhere, with a noticeable saving in the simulation time. Nested domains have a fixed grid increment ratio from a larger domain to the next smaller domain of 1:3.

Grid cell sizes for the RCM were chosen to be compatible with those which would be used when output from a GCM is used to the initial conditions and lateral boundary conditions for the RCM. A previous study of RCM simulation with nested domains indicated that the spatial variability in precipitation increases with the increasing domain resolution (Yu et al., 1999b). In an effort to reduce the computational burden caused by using very high-resolution RCMs, Lakhtakia et al. (1999) conducted a sensitivity analysis with MM5 using three domain set-ups: 36–12–4, 36–12, and 36 km. Their results showed that the 36–12 km nesting generated similar patterns of precipitation and direct surface runoff to those of the 36–12–4 km domain nesting. The 36 km domain set-up produced unrepresentative precipitation distributions in time and space. They concluded that 12 km precipitation fields are a suitable compromise, providing sufficient resolution for simulating the basin response to climate variation and change. Consequently, for this analysis we do not use resolutions finer than 12 km. To promote the eventual linkage of the RCM to a GCM, to minimize the difference in resolution between the RCM and GCM grids, and to achieve acceptable computing time for the

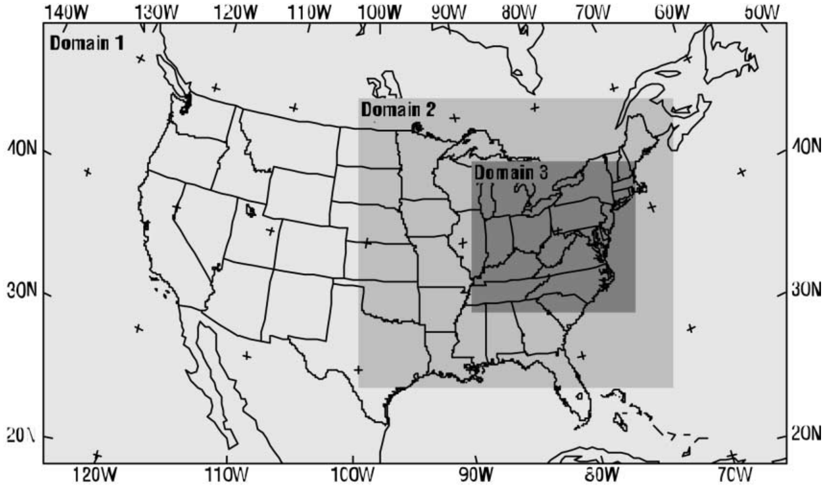

Fig. 1. The three nested domains (108–36–12 km) used in the RCM. Note: Domain 1 is discretized by a mesh of 36 (in the northsouth direction) by 60 (in the westeast direction) grid cells; Domain 2 is discretized by a mesh of 70 by 76 grid cells; Domain 3 is discretized by a mesh of 109 by 118 grid cells.

extended period of the multi-storm simulation, the RCM in the study was set-up with a low resolution domain with a grid increment of 108 km, within which 36 and 12 km domains are nested (108–36–12 km domain set-up) (Fig. 1). Simulations at 4 km grid increments were prohibited by the high computational cost for the multi-storm case in this study. Previous studies suggest that a grid increment of 12 km (tradeoff between using a grid increment of 4 km and required computing time) appears to be sufficient for modeling the hydrologic response to storm events in this region (Lakhtakia et al., 1999; Yu et al., 1999b). Nevertheless, most applications of Susquehanna River Basin Experiment (SRBEX) for short-period single storm events have used nested domains with grid increments as small as 4 km (e.g. Yu et al., 1999a). In those studies, MM5 ran in the non-hydrostatic mode with the multi-level Blackadar-type planetary boundary layer parameterization (Zhang and Anthes, 1982) and Grell cumulus parameterization (Grell, 1993). The smallest grid spacing used here is 12 km but to provide comparability with the earlier work and with future applications with grid increments less than 10 km, we continued to employ the non-hydrostatic mode.

The two-way interactive nesting procedure was used for these applications. Although this procedure is more computer-space and time intensive than the one-way nesting, it prevents the nested domains solutions from diverging (Grell et al., 1995), which was given the relatively long integration times.

MM5 produces outputs of many meteorological variables. The simulated hourly precipitation is the focus of discussion here. MM5 is designed to simulate single storm systems over a few days for weather prediction. To use the model in a climate mode for longer simulations requires non-trivial modifications. One of the two principal adjustments made to MM5 is the addition of a solar radiation scheme because changes in solar forcing over the course of one storm are minor, but over several storms are substantial. To simulate the hydrologic response to atmospheric forcing on time scales ranging from diurnal to interannual and beyond, a critical need of MM5 is to represent the exchange of energy and moisture between the land surface and the atmosphere. This need is especially important in light of the changes in evapotranspiration (ET) that take place over the course of several storms. Consequently, the second essential modification made to the mesoscale model was to couple it to the biosphere–atmosphere transfer scheme (BATS) (Dickinson et al., 1989). As a first step towards our long-term modeling goals, the RCM adapted from MM5 is used to simulate a six-storm sequence for the period of April 22 to May 17, 1981. The modeled and observed multi-storm events are used to drive the HMS for simulating the regional hydrologic response in a subbasin of the Susquehanna River Basin, the Upper West Branch (Fig. 2). For these particular and preliminary applications in this study, RCM is driven by observations, instead of by GCM output, to study the effect that the initial conditions and options with and without BATS have on the modeled precipitation fields, and subsequently on the simulated streamflow hydrograph. The data sets used for defining the initial and temporal lateral boundary conditions for RCM are extracted from the national meteorological center's (NMC) global tropospheric analyses, which have a 2.5° latitude–longitude resolution. The multi-storm simulation used NMC upper-air and surface observations.

3. Hydrologic model system (HMS)

HMS comprises four models or modules, the soil hydrologic model (SHM), the terrestrial hydrologic model (THM), the ground-water hydrologic model (GHM), and the channel ground-water interaction (CGI) model. The overall structure of HMS is described in detail Yu et al. (1999a). HMS utilizes remotely sensed and digital data sets for describing the land characteristics and deriving physical hydrologic parameters. HMS was linked to RCM to simulate the response of the hydrologic system (e.g. streamflow, soil moisture, subgrid-scale spatial variability) to single storm events (Yu et al., 1999a,b). The soil conservation survey curve number (SCS) methods implemented in HMS to partition the available water (sum of precipitation and surface-water routed from the neighboring grid cells) into components of infiltration and surface runoff. This method was successfully used to simulate hydrologic processes (Schaake et al., 1996; Yu et al., 1999a,b).

The model components work interactively to generate flow at the basin outlet. SHM simulates the vertical flow of soil-water by numerically solving the Richards' equation and determines the portion of the computed infiltration that enters the ground-water flow system as recharge (Yu et al., 1999a). The Penman–Monteith method (Monteith, 1981) is implemented for the ET calculation with measured and inferred plant height, leaf-area index, wind speed, and meteorological data. THM employs an algorithm that uses down-slope flow directions to facilitate simulation of overland flow and prediction of surface runoff production. Assuming a linear flow surface across the grid cell, THM applies the kinematic wave method to simulate the overland flow and checks the water balance among the inflow, outflow, and storage for each grid cell at each time step. A channel routing algorithm is used in stream grid cells to route water through the DEM-derived (digital elevation model) channel networks to the simulated basin outlet where the simulated streamflow could be compared to the observed. Infiltration is determined along the overland flow path by applying the overland flow and channel flow routings to each grid cell within the simulated domain for each time step, and by coupling this arrangement with the rainfall-runoff generation schemes. At the end of each time step, the hydraulic gradient between the computed river stages in the channel and simulated ground-water level within the grid cell is used in CGI to calculate the flow flux (or ground-water baseflow) between the channel and the ground-water system (either the ground-water system releasing water to the stream or the stream recharging the ground-water system) (Yu and Schwartz, 1998). GHM (Yu, 1997; Yu and Schwartz, 1998) receives the spatially distributed recharge values from SHM and the spatially varied flow flux on the stream grid cells from CGI and uses them to simulate the transient ground-water configuration at each time step. The simulated ground-water levels are passed to CGI to simulate channel ground-water interaction. The streamflow at the basin outlet consists of components of surface runoff, ground-water baseflow, and direct precipitation fallen on the stream and saturated areas.

4. Subgrid-scale spatial variability

Previous studies of Andre et al. (1986), Entekhabi and Eagleson (1989), and Henderson-Sellers and Pitman (1992), indicate the importance of the subgrid-scale spatial variability when using climate models with distributed hydrologic models to simulate terrestrial hydrologic processes. Using the parameterization schemes of the subgrid-scale spatial variability, the small-scale hydrologic processes at a

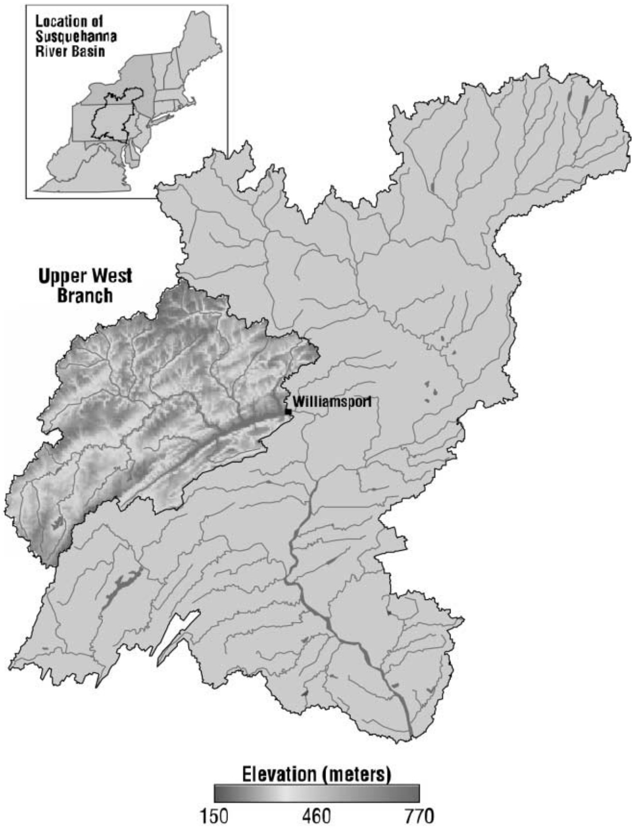

Fig. 2. Location map of the Susquehanna River Basin and its subbasin, the Upper West Branch.

scale of meters can be represented in regional models with a grid scale of kilometers.

Nevertheless, Yu et al. (1999b) show the significant effects that RCM grid resolution and subgrid-scale spatial variability have on the simulated hydrologic variables (e.g. streamflow). The simulated precipitation in RCM represents a single value for each grid cell. This single value over dimension of the order of 10–100 km (and even larger in GCM grids) results in the rainfall that is significantly lower than the actual peak intensities, which is one cause of the underestimation of surface runoff and other variables (Yu et al., 1999a). An additional cause of underestimation is the lack of heterogeneity in soil hydraulic parameters (i.e. saturated conductivity).

Thus, as a first-order approximation to the spatial variability in precipitation and hydraulic parameters, we used the exponential probability distribution to distribute the single value in each RCM grid cell into a set of values (Yu, 2000). The mass conservation is observed during this process. The set of values are then distributed randomly among the subgrid hydrologic cells falling on each RCM grid cell. The subgrid-scale spatial variability in hydraulic parameters (e.g. hydraulic conductivity and soil moisture) was implemented in the hydrologic models. Each hydrologic grid cell is subdivided into many small subgrid fractions and each fraction represents the area having similar hydraulic properties (Famiglietti and Wood, 1994). The exponential probability distribution describes this spatial heterogeneity within each hydrologic grid cell. The rainfall-runoff partitioning procedure is applied to each fraction and the amount of runoff and infiltration is integrated over the hydrologic grid cell to simulate overland flow and soil moisture.

5. Study area

The innermost, high-resolution Domain 3 in the nest used for RCM storm modeling covers much of the eastern United States. Its center is slightly to the west of the Susquehanna River Basin, which covers portions of New York, PA, and MA (Fig. 1). The hydrologic simulation in this study focused on the Upper West Branch, a subbasin of the Susquehanna River Basin (Fig. 2). The Upper West Branch has an area of 14,710 km^2 and flows east into the Susquehanna River. Most of the Upper West Branch lies within the Appalachian Plateau physiographic province, which is characterized as flat upland areas that are deeply dissected by numerous steep-walled, narrow valleys (Yu et al., 1999a). A grid of 190×170 cells with a grid resolution of 1 km was used to discretize the Upper West Branch. All the surface and subsurface hydrologic parameters were gridded to this resolution, while analyzed observed and modeled precipitation fields were downscaled to the resolution of 1 km for the hydrologic simulation. The hourly observed precipitation data were interpolated to the RCM and HMS domains following the analysis method of Haagenson et al. (1992) (Yu et al., 1999a).

6. Hydrologic data sets

A major part of the work involved compiling, integrating, and preparing the physiographic, soil, land use, hydrological, and meteorological data for the simulations of hydrologic processes: ET, infiltration, overland flow, ground-water flow, and channel ground-water interaction. Available remotely sensed information, such as vegetation type and derived seasonal fractional vegetation cover, were used. Detailed information about derivation and manipulation of various data sets is described in previous papers (Yu et al., 1999a).

The DEM for the study area is derived from US geological survey (USGS) 3-arc second data. For this study, the DEM was generalized to the same grid scale and map projection as the precipitation and the other data sets and was used for determining the drainage area, the flow direction, the aspect ratio, the basin boundary, and the stream network (Yu et al., 1999a). Hydrologic parameters (e.g. conductivity and SCS curve number) are derived from the state soil geographic (STATSGO) soils data (Miller and White, 1998). The method of Rawls and Brakensiek (1985) is used to estimate the various hydraulic parameters for different soil textures (e.g. capillary suction). Land use and land cover data are derived from AVHRR satellite imagery of the EROS data center (EDC).

The 12 km RCM-simulated hourly precipitation is downscaled to the 1 km hydrologic model grid to drive HMS for the hydrologic simulation. While different types of HMS output are available (e.g. runoff, infiltration, ground-water baseflow), the focus of hydrologic analysis here is on the streamflow at the basin outlet.

7. Model calibration

Complexity in simulating the hydrologic response in large watersheds over long times has prompted a significant need for a rigorous calibration procedure. Beven and Binley (1992) described a procedure of model calibration and uncertainty prediction. Yu and Schwartz (1999) implemented a calibration procedure in a physically-based distributed-parameter watershed model for the simulation of surface-water/ground-water interaction. Following the procedure of Yu and Schwartz (1999), the calibration of the HMS in the Upper West Branch and other subbasins has made use of the digital and remotely sensed data sets, measured precipitation, soil moisture, ground-water level, and streamflow data that are available for the various locations within the Susquehanna River Basin (Yu et al., 1999a,b). The calibration process emphasized adjusting the estimated values of surface and subsurface key hydraulic parameters (e.g. conductivity, storativity, streambed permeability) until HMS give a good overall fit to measured values at a number of locations throughout the basin. The hydraulic parameters were adjusted to optimize various objective functions or fitness measures (equivalent to the minimization of the sum of squares of the residuals). Mean error, mean absolute error, and root mean squared error between simulated results and observed data are used to evaluate the simulation performance. The two-stage model calibration, a steady-state stage (100 days) followed by a transient stage (few weeks to months), was used with HMS. The steady-state stage is driven by the average observed meteorological records, while the transient stage by the daily-observed meteorological records. The first stage employs model balancing among various hydrologic components to eliminate the effect of unrealistic initial conditions on the simulation in various submodels and to reach an equilibrium condition among models, given initial conditions and external forcing. Various initial conditions are optimized as the starting condition for the hydrologic simulation by comparing the overall simulated response with observation (e.g. streamflow and baseflow) at the transient stage of the calibration procedure.

THM was used to simulate the overland flow and channel flow of a 7.3 km^2 watershed within the Susquehanna River Basin. The model was calibrated to this watershed. Sensitivity analysis was conducted to examine the effect of various initial abstraction conditions of soil moisture on the rainfall-runoff partitioning and the effect of Manning roughness on the overland flow simulation. Sensitivity analysis on parameters derived from the historical record of streamflow data, which are related to channel flow were also conducted on this watershed and the Upper West Branch. The results indicate that the accurate simulation of overland flow and channel flow plays a significant role in shaping the hydrograph and determining the peak timing and maximum discharge value which have implications on the flooding forecast (Yu et al., 1999a). The larger the watershed, the more important the channel flow routing and the less important the overland flow routing, and vice versa.

Simulated soil moisture was also calibrated to the 75-day field observed data within the Upper West Branch and other subbasins within the study area (Yu et al., 2000) while the ET calculation followed the Penman–Monteith method (Monteith, 1981) by using measured parameters (e.g. measured plant height, leaf-area index, wind speed, fractional vegetation cover). The simulation compares well with the observation in terms of fit in the daily variation and seasonal trend. The calibrated model was used to evaluate the effect of soil texture and land use on the water balance among various hydrologic components such as runoff, ET, soil moisture deficit, and ground-water recharge.

The observed streamflow hydrograph was separated into components of surface runoff and ground-water baseflow using a modified version of a hydrograph separation method (Yu and Schwartz, 1999). The estimated runoff and baseflow are part of targets in the calibration process and compare well with simulated ones. The overall streamflow matches with the observed at Williamsport, PA, the outlet of the Upper West Branch; while the temporal variation in ground-water level is comparable to the general trend of observed ground-water level in wells within the watershed (Yu et al., 1999a). No exhaustive calibration is performed to match the spatial distribution of ground-water level at this stage because of the lack of available data. This problem is being addressed by an ongoing study, which seeks to estimate the parameters in the ground-water system by using the spatially distributed ground-water level and field well testing results. The simulation results of previous research indicate that the model is well calibrated. The calibrated HMS has successfully simulated the hydrologic response to precipitation generated by various storm systems, including analyzed observed precipitation and MM5-simulated precipitation (Yu et al., 1999a,b). In this study, the calibrated HMS is applied to six successive storms. Simulated soil moisture is used as the antecedent moisture condition before each storm to interpolate the curve number for rainfall-runoff partitioning.

8. Results

RCM simulated six-storm events that occurred from 1200 UTC April 11 to 0000 UTC May 17, 1981; while the hydrologic simulation started at the same time as the RCM and ended five days later than the RCM simulation to capture the streamflow response of the last storm event. The aim of the research was to assess the ability of HMS to simulate six successive storms accurately. None of the six-storms is anomalous and each storm is discrete in time and space. The storm simulation section provides descriptions of the storms, details of the storm simulations, and sensitivity analyses of various grid-nesting schemes, initial moisture conditions, and atmosphere-land surface interactions. Then the following sections contain the hydrologic simulation with observed precipitation fields followed by the results of the RCM multi-storm simulation and the hydrologic simulation with RCM-modeled precipitation fields. While there are many simulated variables in HMS, we focused here on the overall hydrologic response of HMS, as represented by streamflow at the basin outlet, to both analyzed observed and simulated precipitation fields associated with the six-storms. The HMS-simulated streamflow is generated every 10-min because the 10 min time step was used in the hydrologic simulation.

8.1. Storm simulation

Ten six-storm simulations were performed and the sensitivity of the simulated precipitation were tested to four factors, including (1) the configuration of nested grids, (2) the presence or absence of BATS, (3) the initial surface moisture conditions specified in the model, and (4) possible model drift. Six-storms that occurred between 1200 UTC April 11 and 0000 UTC May 17, 1981 were simulated. The storms were chosen primarily for hydrologic, rather than atmospheric, reasons; that is, mid-spring storms simplify the initial conditions of the hydrologic model because snow cover is absent, soil-water content tends to be moderate to high, and ET is relatively low (Yu et al., 1999a). The storms and the results of the sensitivity analyses are summarized here.

Storm 1 formed on 20 April 1981 in the lee of the Canadian Rocky Mountains of Alberta. The wave cyclone migrated west and by early on 23 April dragged a cold front across the SRB. Rain peaked twice the larger peak coming from the initial cold front passage and the smaller peak from the trailing instability showers. Coincident with the cold front passage of Storm 1 on 24 April, Storm 2 formed in the lee of the Rocky Mountains in eastern Montana. The storm slowly migrated through the northern United States, finally exiting the continent through the Canadian Maritimes on 30 April. Precipitation started over the SRB on 28 April and persisted for nearly two days, consisting of three clear peaks, which corresponded to the passage of the warm front, cold front, and trailing occlusion. Storm 3 was an upper level trough that moved from the northwest and passed over the SRB on 2 May. The trough proceeded to deepen and to advance to the southeast, where it became a cut-off low spinning off the Carolina coast through 6 May. Precipitation from the 2 May trough was the least of the six-storms in the sequence. Storm 4 resulted from a low-pressure center that traversed central Quebec. Its trailing cold front passed over the SRB, bringing a brief, prefrontal instability shower on 5 May, as well as a heavier rainstorm on 6 May. Storm 5 was the most powerful of the six-storms, dragging a cold front over the SRB from 11 to 13 May and bringing a heavy two-day rainstorm. Storm 6 was a classic Colorado Low that passed just to the northwest of the SRB a few days later and produced an archetypal warm front, cold front, and cool-air-instability shower sequence of precipitation.

The sensitivity analyses demonstrated the importance of nesting and of atmosphere-surface interaction. First, the 108–36–12 km nesting did not provide results that were noticeably different or better than the 108–36 km nesting. That finding, however, does not negate the importance of nesting. The results showed that interactively nesting the 36 km domain within the 108 km domain dramatically improved simulation results and reduced computational time when compared to the unnested 36 km simulation. Second, the sensitivity analysis found that precipitation was intensified when initial soil moisture was greater, especially when BATS was used. Nevertheless, the differences between the drier and wetter, no-BATS and BATS cases were not great. Third, the results showed that—for any individual storm—the inclusion of BATS did not affect the simulation substantially. Slightly higher precipitation rates were found with the inclusion of BATS. Fourth, our 'late start' simulations proved, nevertheless, that the inclusion of BATS is critical to the success of multi-storm simulations. The no-BATS simulations drifted considerably as the number of storms rose; in contrast, the BATS simulations simulated each storm accurately in time and space.

In the end, results demonstrated that the modified version of MM5 could successfully simulate a multi-storm sequence. Importantly, they confirmed that the cumulative feedbacks of mass and energy between the surface and atmosphere are critical components of storm trajectory, evolution, and intensity. Without a soil-vegetation-atmosphere transfer (SVAT) scheme such as BATS, multi-storm simulations of spatially distributed precipitation will drift increasingly away from the targeted areas over time.

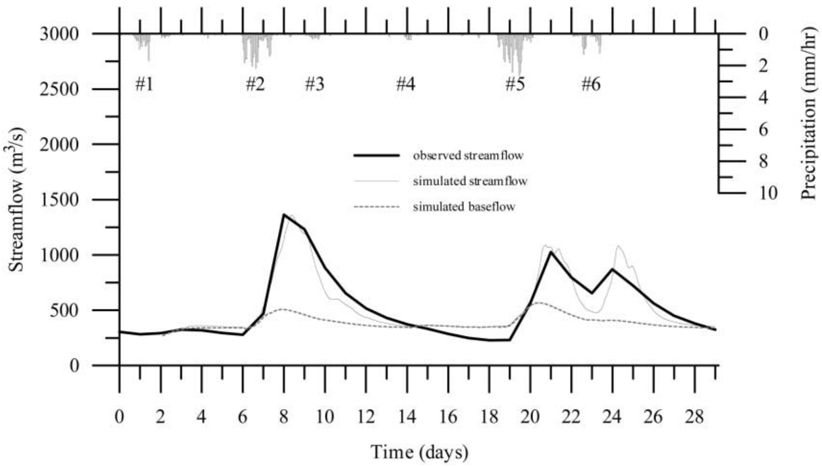

Fig. 3. Observed and HMS-simulated streamflow with analyzed observed precipitation.

8.2. Hydrologic simulation with analyzed observed precipitation

The hydrologic simulation with observed precipitation was conducted to reproduce the hydrologic response to the six-storm sequence during the period of April 11 to May 21, 1981. Shown in Fig. 3 are observed and simulated flow hydrographs along with the analyzed areally averaged observed precipitation. The daily streamflow data are from the USGS gauge station at Williamsport, PA. The streamflow consists of components of surface runoff and ground-water baseflow. The average hourly precipitation rates were approximately 1.5 mm/hr; no hourly readings exceeded 4 mm/hr.

Due to the low intensity of precipitation rates for the first storm and a period of no rain before this event, no significant runoff was generated during this event. In other words, most precipitation infiltrated the surface and recharged the soil, with only minor amounts recharging the ground-water system. Consequently, only a slight increase in the ground-water baseflow was observed days after the precipitation event. However, because this first event satisfied the moisture deficit in the soil column, when combined with the saturated soil, the relatively high precipitation rates of the second storm event were able to produce a significant increase in both surface runoff and ground-water baseflow.

HMS considered the runoff generated due to the soil saturation, but still slightly underestimated the runoff for several reasons. Some of these reasons relate to the relatively large grid size used to discretize the HMS domain. Small-scale effects that take place during the storm event, such as bank storage and expansion of near-stream saturation areas (Yu et al., 2000) during the storm event could not be explicitly described in the model and this will underestimate the surface runoff. The grid size also affects the ground-water flow simulation. In order to calibrate the simulation to the observation, one tends to over parameterize hydraulic variables (e.g. hydraulic conductivity and storativity) in the ground-water system. This over parameterization results in selection of conductivity values that are on the high end of the plausible range. Another problem is that, during the storm event, the simulated peak of ground-water baseflow arrives a little earlier than expected and the baseflow recession is slow. Although it is possible to tune the parameters to obtain a better match between the simulation and observation, the optimized value of parameters will fall out of the plausible range. Such values are referred as 'effective' values of related hydraulic parameters. The improved performance of the calibration with this practice does not necessarily imply improved understanding of the physical processes. Instead, the improvement of the subgrid-scale spatial and temporal variability, which is based on understanding how the subgrid-scale variability affects the physical processes within a grid cell, should be

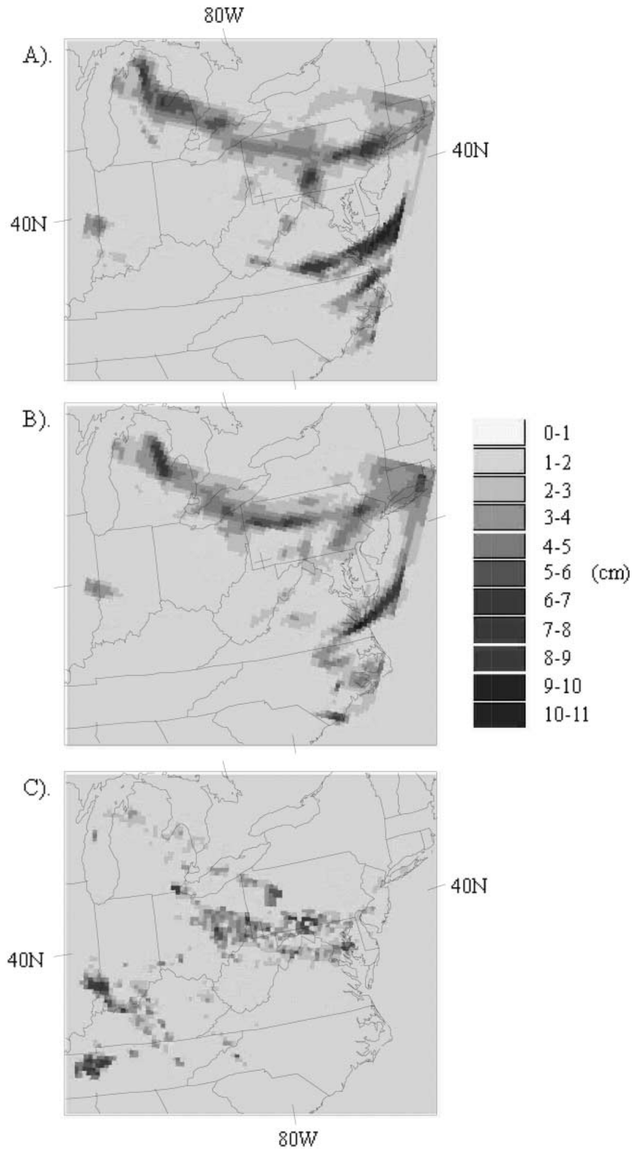

Fig. 4. Spatial distribution of the temporally integrated RCM-modeled and analyzed observed precipitation in the 12 km grid domain ((a) With BATS; (b) Without BATS; (c) Observed). Note: the latitude and longitude of four corners are northwest (46.284° north latitude, 88.361° west longitude); northest (43.749°, 70.332°); southwest (34.427°, 89.541°), southeast (32.372°, 74.520°).

implemented in the system to capture the response (Beven, 1989; Henderson-Sellers and Pitman, 1992; Yu et al., 1999a).

The simulated response to the third storm event can be observed on the falling limb of the hydrograph while no response to such storm was recorded on the observed hydrograph. Because there is a dry period, which followed the third storm, the hydrologic response to the fourth storm event is neither observed nor simulated in the streamflow hydrograph.

Although the precipitation rates of the fifth storm event were high, the substantial dry period that followed the fourth storm suppressed both the observed and simulated hydrologic response and the

Table 1
Summary of analyzed observed and simulated stormed events(unit in mm)

	#1	#2	#3	#4	#5	#6
Observed	12.0	30.1	3.4	2.6	35.9	10.7
With bats	28.0	28.9	1.3	21.1	2.3	2.42
Without bats	32.7	37.7	0.2	9.9	9.7	13.0

simulated streamflow hydrograph is smaller than the response to the second storm. For the fifth and sixth storms, the HMS-simulated streamflows generally matched as well with the observed timing, hydrograph peak values, and ascending and descending limbs of the hydrograph as other previous storms. As we expect, the calibrated model was able to reproduce the observed events (e.g. the timing of hydrograph peaks was well captured by the simulation).

8.3. Hydrologic simulation with RCM-modeled precipitation

As noted earlier, extensive sensitivity analyses of the six-storm RCM simulations were performed. The 37 day RCM simulation was conducted to model the multi-storm events, starting at 1200 UTC April 11, 1981. The RCM simulations with various set-ups were designed to conduct the sensitivity analysis. Here, we used one of their more accurate simulations—a 108–36–12 km nesting using BATS and initialized with moderate soil moisture conditions—to provide precipitation input for the HMS simulation of the six-storm sequence. Note that we performed simulations for most of their 10 RCM simulations and found the ability of HMS to simulate the Upper West Branch response to be comparable in all cases.

The spatial distribution of RCM-simulated precipitation accumulated in the 12 km domain over the entire six-storm simulation period is shown in Fig. 4 along with the analyzed observed precipitation field. Fig. 4 shows the distribution of RCM simulations with and without BATS. Although the RCM simulation did capture the storm pattern, there are still significant differences between the simulated and analyzed observed precipitation fields. The range of simulated precipitation (0–10 cm with BATS and 0–10.4 cm without BATS) is higher than the observed (0–9 cm). For this and other RCM simulations (not shown), RCM overestimated the total amount of precipitation in time and space and had more wide-spreading storm patterns compared to the analyzed observed rainfall for the six-storm period. Part of this discrepancy could be attributed to the density of the raingage network; i.e. the 12 km grid spacing of the simulated rainfall is much finer than the precipitation observations. There are some small differences in the spatial distribution between the RCM simulations with and without BATS and there are differences in the temporal variations; these will be discussed later.

The simulated six-storm events with BATS and without BATS were summarized in Table 1. In general, each storm event was captured in simulations while the

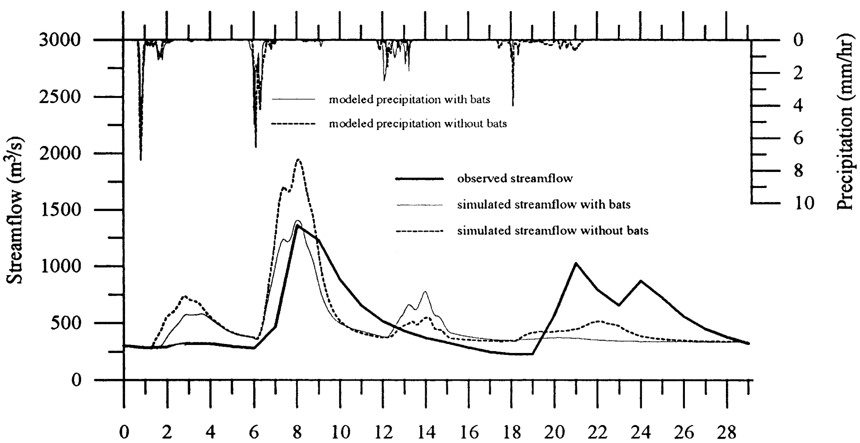

Fig. 5. HMS-simulated streamflow with RCM-modeled precipitation with and without BATS.

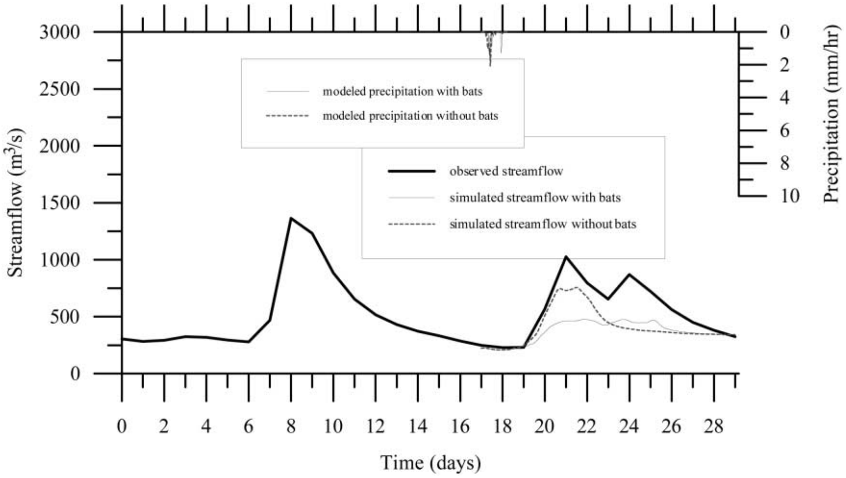

Fig. 6. HMS-simulated streamflow with RCM-modeled precipitation with a late start.

discrepancy exists in rainfall intensity. The RCM-simulated hourly precipitations with BATS and without BATS were downscaled to the hydrologic model grid with a resolution of 1 km and were used to drive HMS for the hydrologic simulation. The simulated streamflow hydrographs are plotted in Fig. 5 along with the areally averaged precipitation. The simulated temporal timing and intensity of the precipitation events are similar between the two RCM simulations with and without BATS. The RCM simulation without BATS produces more precipitation than the RCM simulation with BATS. This difference is reflected on the simulated streamflow hydrographs. Compared with the analyzed observed precipitation, the RCM simulation significantly overestimated the amount and intensity of precipitation for the first storm event (Table 1). The RCM simulation with BATS was able to reasonably capture the second storm, but the event arrived hours early. The peak of the RCM-modeled third storm arrived at about the same time as observed, while the simulation without BATS almost missed the storm event. These small storm events did not produce any noticeable change on the hydrograph. The modeled fourth storm is much larger than the observed, resulting in a peak on the hydrograph and high recessed ground-water baseflow. The RCM simulated fifth and sixth storms with BATS and without BATS compares poorly with the observed ones in time and intensity (Table 1). This results in a significant underestimation in streamflow amount and peak value and timing (Fig. 5).

Overall, although the RCM simulation captured the signals of storms, the magnitude of these events was poorly simulated. Subsequently, the HMS simulation with the RCM-modeled precipitation was not able to reproduce accurately the streamflow hydrograph at the basin outlet. These results show the limited value of applying such RCM simulations to hydrologic application at this scale. Part of the reason is the size of the Upper West Branch (14,710 km^2). The overall statistics of precipitation within Domain 1 of RCM indicate that the larger the size, the closer the modeled precipitation to the observed. The results do show that the RCM simulation with BATS seems to do a better job than the RCM simulation without BATS. A previous study (Yu et al., 1999a) shows that the RCM simulation simulates the single storm event well. In the current experiment, the RCM simulation degrades with the time. Part of this degradation is due to the small size of basin, the spatial heterogeneity of the storms, and the time scale beyond the model prediction in a climate mode. Further research is required to conduct and evaluate more RCM simulations on multi-storm events. So the generalized sequence of synoptic storm events can be developed and statistical downscaling can be used more effectively to downscale the mesoscale precipitation to the resolution of the fine-scale hydrologic model for the basin hydrologic applications. So the characteristics of storm events can be preserved in any particular basin within the RCM domain.

Sensitivity analysis was conducted to evaluate how the initial soil condition affects the RCM simulation. Two RCM simulations with a wet start with and without BATS were performed. Although six-storm events can be discerned in these two RCM simulations, the magnitude of the storm events is significantly reduced and the resulting streamflow hydrographs compare poorly with the observed (not shown).

Previous studies indicate that the RCM performs well in the single storm simulation. To find out whether the data could play any role in the mismatch on the later storm events (fifth and sixth) in the RCM simulation, two RCM simulations with a late start (starting a day before the fourth storm event) was conducted. The simulated results were improved (Fig. 6). This suggests that the underestimation of storm events could be due to the errors in degraded lateral and temporal meteorological conditions when it changes from a weather mode to a climate mode.

9. Conclusions

This paper presents the use of a HMS to simulate the basin-scale hydrologic response to precipitation from a series of storms. The precipitation inputs that drove HMS came from analyses of observations and from a RCM. Observed initial and lateral boundary conditions drove the RCM storm simulation. The procedure eventually will facilitate the use of a GCM to provide the boundary conditions for RCM simulation and for the RCM to drive the simulation of regional hydrologic processes. In other words, the model system should someday simulate the local basin response to global climate forcing.

Nevertheless, the results indicate that the model system is not ready for that step. Experimental runs show that the match between simulated and observed streamflow during the dry period could be further improved by using unrealistic values of hydraulic parameters (e.g. hydraulic conductivity and storativity), which are out of the plausible range. In general, the HMS response to observed precipitation compared well with observed streamflow at the basin outlet, and the results suggested that the model was well calibrated. However, careful inspection of individual hydrographic traces indicated that important scale-induced discrepancies exist.

The RCM-modeled precipitation fields with BATS and without BATS were used to drive the HMS simulation. The RCM simulation with BATS performs slightly better than the RCM simulation without BATS, although even using BATS there are discrepancies in space and time between simulation and observation. More important, although the RCM six-storm simulation captured general precipitation patterns well, there were significant spatial and temporal differences when simulated and analyzed precipitation fields were compared in detail. These differences are due to the size of the storm, the nature of spatial variability, and the change from a single storm simulation in a weather mode to the multi-storm simulation in a climate mode. These discrepancies naturally resulted in divergent simulated streamflow.

RCM simulations with a start of wet soil moisture and a late start were also conducted to evaluate how the initial soil moisture condition affects the simulation and how the cumulative feedbacks of mass and energy between the surface and atmosphere degrade the multi-storm simulation. The RCM storm simulation performs less well as soil moisture increases. Also, the RCM simulation with a late start simulated the later storms more accurately and, consequently, the HMS simulation of streamflow response is improved.

The results are still encouraging. Our work suggests that continued improvements in model physics and parameterizations will enable scientists one day to simulate precipitation and basin response weeks in advance. More analysis is required to develop a genetic sequence of synoptic storm events based on records of historical storm events. Then the simulated storm events can be statistically downscaled to fine hydrologic scale for the basin-scale hydrologic simulation. We are currently testing our new fully coupled system of GCM, RCM, and HMS. This system will be used to conduct seasonal climate and hydrologic simulations at a continental scale and various basin-scales in the near future. So an optimal scale can be found when it is appropriate time to use a deterministic or a stochastic downscaling approach to downscale the RCM-modeled precipitation to the resolution of the fine-scale hydrologic model for the hydrologic analysis and applications.

Acknowledgements

This study was funded by NASA (1779-UNLV-NASA-4553 and Global Water Cycle: Extension Across the Earth Sciences: NASA EOS, NAGW-4553).

References

Andre, J.C., Goutorbe, J.P., Perrier, A., 1986. HAPEX-MOBILHY: a hydrologic atmospheric experiment for the study of water budget and evaporation flux at the climatic scale. Bull. Am. Meteorol. Soc. 67, 138–144.

Beven, K., 1989. Changing ideas in hydrology—the case of physically based models. J. Hydrol. 105, 157–172.

Beven, K., Binley, A., 1992. The future of distributed models: model calibration and uncertainty prediction. Hydrol. Process. 6, 43–69.

Dickinson, R.E., Errico, R.M., Giorgi, F., Bates, G.T., 1989. A regional climate model for the western United States. Clim. Change 15, 383–422.

Dudhia, J., 1993. A nonhydrostatic version of the Penn State-NCAR mesoscale model: validation tests and simulation of an Atlantic cyclone and cold front. Mon. Weath. Rev. 121, 1493–1513.

Entekhabi, D., Eagleson, P.S., 1989. Land surface hydrology parameterization for atmospheric general circulation models including subgrid scale spatial variability. J. Clim. 2, 816–831.

Famiglietti, J.S., Wood, E.F., 1994. Multiscale modeling of spatially variable water and energy balance processes. Water Resour. Res. 30, 3061–3078.

Grell, G.A., 1993. Prognostic evaluation of assumptions used by cumulus parameterizations. Mon. Weath. Rev. 121, 764–787.

Grell, G.A., Dudhia, J., Stauffer, D.R., 1995. A description of the fifth-generation Penn State/NCAR Mesoscale Model (MM5), NCAR/TN -398 + IA.

Haagenson, P.L., Gill, D.O., Kuo, Y.-H., 1992. Real-time forecasts for WISP-91 using the Penn State/NCAR Mesoscale Model, NCAR/TN-380 + STR.

Henderson-Sellers, A., Pitman, A.J., 1992. Land-surface schemes for future climate models: specification aggregation of heterogeneity. J. Geophys. Res. 97, 2687–2696.

Kattenberg, A., Giorgi, F., Grassl, H., Meehl, G.A., Mitchell, J.F.B., Stouffer, R.J., Tokioka, T., Weaver, A.J., Wigley, T.M.L., 1996. Climate models—projections of future climate in climate change 1995. In: Houghton, J.T., Meira Filho, L.G., Callander, B.A., Harris, N., Kattenberg, A., Maskell, K. (Eds.). The Science of Climate Change. Cambridge University Press, Cambridge, pp. 285–357.

Kunkel, K.E., 1996. A hydroclimatological assessment of the rainfall. In: Changnon, S.A. (Ed.). The Great Flood of 1993: Causes, Impacts, and Responses. Westview Press, Boulder, CO, pp. 52–67.

Lakhtakia, M.N., Yu, Z., Yarnal, B., White, R.A., Miller, D.A., 1999. Sensitivity of simulated surface runoff to mesoscale meteorological model resolution in a linked-model experiment. Clim. Res. 12, 15–27.

Leung, L.R., Ghan, S.J., 1999. Pacific northwest climate sensitivity simulated by a regional climate model driven by a GCM Part II: 2XCO2 simulations. J. Clim. 12, 2031–2053.

Leung, L.R., Wigmosta, M.S., Ghan, S.J., Epstein, D.J., Vail, L.W., 1996. Application of a subgrid orographic precipitation/surface hydrology scheme to a mountain watershed. J. Geophys. Res. 101, 12,803–12,817.

Leung, L.R., Hamlet, A.F., Lettenmaier, D.P., Kumar, A., 1999. Simulations of the ENSO hydroclimate signals in the Pacific northwest Columbia River basin. Bull. Am. Meteorol. Soc. 80, 2313–2329.

Miller, N.L., Kim, J., 1996. Numerical prediction of precipitation and river flow over the Russian River watershed during the January 1995 California storms. Bull. Am. Meteorol. Soc. 77, 101–105.

Miller, D.A., White, R.A., 1998. A conterminous United States multi-layer soil characteristics data set for regional climate and hydrology modeling. Earth Interact. 2.

Monteith, J.L., 1981. Presidential address: evaporation and surface temperature. Q. J. R. Meteorol. Soc. 107, 1–28.

Rawls, W.J., Brakensiek, D.L., 1985. Prediction of soil-water properties for hydrologic modeling, in watershed management in the eighties. Am. Soc. Civ. Engng, 293–299 New York.

Schaake, J.C., Koren, V.I., Duan, Q.Y., Mitchell, K., Chen, F., 1996. Simple water balance model for estimating runoff at different spatial and temporal scales. J. Geophys. Res. 101, 7461–7475.

Yu, Z., 1997. Application of vector and parallel supercomputers on groundwater modeling. Comput. Geosci. 23, 917–927.

Yu, Z., 2000. Assessing the response of subgrid hydrologic processes to atmospheric forcing with a hydrologic model system. Global Planet. Change 25, 1–17.

Yu, Z., Schwartz, F.W., 1998. Application of integrated basin-scale hydrologic model to simulate surface water and ground-water interactions in Big Darby Creek Watershed, Ohio. J. Am. Water Res. Assoc. 34, 409–425.

Yu, Z., Schwartz, F.W., 1999. Automated calibration applied to constrained ground-water flow modeling. Hydrol. Process. 13, 191–209.

Yu, Z., Lakhtakia, M.N., Yarnal, B., White, R.A., Miller, D.A., Frakes, B., Barron, E.J., Duffy, C., Schwartz, F.W., 1999a. Simulating the river-basin response to atmospheric forcing by linking a mesoscale meteorological model and a hydrological model system. J. Hydrol. 218, 72–91.

Yu, Z., Lakhtakia, M.N., Barron, E.J., 1999b. Modeling the river-basin response to single-storm events simulated by a mesoscale meteorological model at various resolutions. J. Geophys. Res. 104 (D16), 19,675–19,690.

Yu, Z., Gburek, W.J., Schwartz, F.W., 2000. On evaluating the spatial distribution of water balance in a small watershed, Pennsylvania. Hydrol. Process. 14, 941–956.

Zhang, D.-L., Anthes, R.A., 1982. A high-resolution model of the planetary boundary layer-sensitivity tests and comparisons with SESAME-79 data. J. Appl. Meteorol. 21, 1594–1609.